INTERNATIONAL JOURNAL OF ENERGY STUDIES

e-ISSN: 2717-7513 (ONLINE); homepage: https://dergipark.org.tr/en/pub/ijes

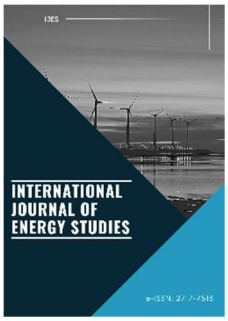

Research Article
Int J Energy Studies 2024; 9(2): 199-218
DOI: 10.58559/ijes.1420875

Received : 17 Jan 2024
Revised : 21 May 2024
Accepted : 05 June 2024

Machine learning predictions and optimization for thermal energy storage in cylindrical encapsulated phase change material

Burak İzgi*

[*]Department of Mechanical Engineering, Yozgat Bozok University, Yozgat, Türkiye, ORCID: 0000-0001-9491-8653
*(*Corresponding Author:burak.izgi@bozok.edu.tr)*

Highlights

- A machine learning model was developed to predict the total melting time of phase change material.
- The Multi Layer Perception model outperforms with 4.07% mean absolute percentage error, showcasing its precise predictive capability.
- Multi-objective optimization was conducted to optimize both stored energy and power.
- Non-dominated Sorting Genetic Algorithm (NSGA-II) optimization highlights trade-offs between stored energy and power, guiding balanced design.

You can cite this article as: İzgi B. Machine learning predictions and optimization for thermal energy storage in cylindrical encapsulated phase change material. Int J Energy Studies 2024; 9(2): 199-218.

ABSTRACT

Accurate prediction of melting time is crucial in designing Thermal Energy Storage (TES) systems based on cylindrically encapsulated Phase Change Materials (PCMs). The melting time of a cylindrical encapsulated PCM directly correlates with the energy stored in the system. This study introduces a precise prediction model for the total melting time of cylindrically encapsulated PCM, utilizing a machine learning algorithm. The model, developed with the Multilayer Perceptron (MLP) method, demonstrated superior performance compared to the correlation equation proposed in the literature. The Mean Absolute Percentage Error (MAPE) value for the correlation equation was 16.68%, while the MLP model achieved a significantly lower MAPE of 4.07%, indicating its success in capturing the intricate relationship between input parameters and melting time. Furthermore, optimization results using the Non-dominated Sorting Genetic Algorithm II (NSGA-II) underscore the importance of striking a balance between stored energy and power during the design process. Maximizing stored energy (81.78 kJ) minimizes power (12.69 W), and vice versa, maximizing power (73.38 W) minimizes stored energy (37.10 kJ). In the case of equal weighting for stored energy and power in the design (56.05 kJ and 38.89 W, respectively), a 31.5% decrease in energy and a 206.5% increase in power were observed compared to the scenario where energy is maximized. Additionally, a 44% decrease in power and a 51.1% increase in energy were noted compared to the case where power is maximized. These findings collectively highlight the robustness and effectiveness of the developed MLP model in accurately predicting melting time and providing optimal solutions for energy storage parameters.

Keywords: Thermal energy storage, Phase change materials, Machine learning, Optimization

1. INTRODUCTION

Thermal energy storage (TES) is crucial for managing the variability of renewable energy sources and improving the overall efficiency of energy systems [1]. By allowing the decoupling of energy generation and consumption, TES enables the storage of excess thermal energy during periods of surplus production for later use during high demand or low generation periods. This flexibility contributes to grid stability, mitigates the impact of variable energy sources like solar and wind, and supports the integration of renewable energy into existing infrastructures [2]. Moreover, TES systems empower industries to optimize energy consumption, manage peak loads, and improve process efficiency, resulting in reduced operational costs and environmental impact. Beyond its immediate applications, the importance of thermal energy storage extends to its role in promoting energy resilience, offering a viable solution for meeting energy demands [3] in diverse sectors, from residential and commercial spaces [4,5] to industrial processes and power plants [6,7]. As the world transitions towards sustainable and resilient energy systems, the significance of TES emerges as a key enabler for achieving a cleaner, more reliable, and economically viable energy landscape [8].

Phase change materials (PCMs) stand as integral components in thermal energy storage systems, offering unique advantages that enhance the efficiency and versatility of energy storage technologies [9]. The distinctive feature of PCMs lies in their ability to absorb or release latent heat during phase transitions, providing a highly efficient and compact means of storing thermal energy [10]. By harnessing the latent heat associated with the transition between solid and liquid states, PCMs enable the storage of substantial amounts of energy within a narrow temperature range. This characteristic makes them particularly valuable in applications where maintaining a stable temperature is critical, such as building climate control [11] and electronics cooling [12]. Additionally, the isothermal nature of phase transitions in PCMs minimizes temperature variations during the energy release process, contributing to enhanced system performance.

Macro-encapsulation stands out as a prevalent and practical technique in the containment of PCMs. This method involves enclosing the PCM within a larger structure, forming a distinct and manageable unit. The encapsulation material, often selected for its compatibility with the PCM and desired thermal properties, serves as a protective barrier, preventing leakage and facilitating the controlled release of thermal energy during phase transitions [13]. PCMs encapsulated in vertical cylinders represent a specialized and efficient approach to thermal energy storage. This

design capitalizes on the cylindrical geometry to optimize space utilization and facilitate efficient heat transfer. The encapsulation of PCMs within the vertical cylinder allows for a higher surface-to-volume ratio, promoting enhanced heat exchange between the PCM and its surroundings. This configuration proves advantageous in various applications, such as solar heating systems and waste heat recovery, where the efficient storage and release of thermal energy are paramount. The vertical alignment supports natural convection processes within the PCM, facilitating uniform phase change [14].

In existing literature, numerous studies explore experimental, numerical, and analytical investigations into PCM melting inside a cylindrical tube. Previous studies have commonly focused on the melting process, fluid flow, and heat transfer characteristics of the phase change process [15–18]. Jones et al. [19] conducted experimental measurements while observing the melting process of n-eicosane, acting as a PCM with a moderate Prandtl number, within an invertedly heated cylinder. They visually recorded the melting front through photography and determined its position using digital image processing techniques. Fraiman et al. [20] performed experiments utilizing vertical tubes of four varying diameters, filled with PCM and immersed in a water bath. The study investigated three PCM heights corresponding to each tube diameter. Experiments were conducted at different water bath temperatures—10, 20, and 30°C above the PCM's melting temperature. The design of the study allowed for a systematic examination of the influence of tube dimensions, PCM heights, and water bath temperatures on the melting behavior of the paraffin within the vertical tubes. In the study conducted by Malya et al. [21], a comprehensive parametric scaling investigation was undertaken. The researchers explored a diverse range of radii and wall temperatures, systematically varying these parameters to analyze their impact on the thermal behavior of the cylindrical encapsulated PCM system. In addition to the studies on the melting of PCM, some research has suggested correlations for predicting the total melting time [16,20,21].

Employing machine learning techniques represents a novel strategy to minimize the expenses and computational time associated with studies. Consequently, these methods have found widespread application in various industrial thermal engineering domains, including evaluating heat exchanger performance [22], predicting two-phase flow patterns [23], and addressing thermal energy storage applications [24,25]. Despite their extensive use in diverse areas, machine learning methods are infrequently applied to predict the melting time of PCMs [26,27].

The melting time of a cylindrical encapsulated PCM is directly related to the energy stored in the system. Accurate prediction of the melting time is crucial in designing TES systems based on cylindrically encapsulated PCMs. The melting time of PCM for use in a TES system can be determined experimentally or using computational fluid dynamics (CFD). However, it can be costly and time-consuming to conduct experiments for each different geometrical parameter when the encapsulation dimensions vary. Similarly, as the number of geometric parameters to be tested increases, CFD solutions become more expensive in terms of computational time. Additionally, it is not feasible to test all alternative designs, either experimentally or via CFD, to achieve an optimal design. Therefore, an accurate and fast model is needed to immediately observe the effect of design changes on PCM melting time and to determine the optimum design. The originality of this work lies in the development and implementation of a machine learning model to predict the total melting time of vertically oriented, cylindrically encapsulated PCM, and in optimizing the geometrical and thermal parameters using the developed machine learning model along with a genetic optimization algorithm.

This paper presents a machine learning model that accurately and quickly predicts the melting time of vertically oriented, cylindrically encapsulated PCM using previously published experimental data. Furthermore, it details the optimization results of the geometrical and thermal parameters using the developed machine learning model and the NSGA-II genetic algorithm optimization method.

2. METHOD

In this study, an accurate prediction model for the total melting time of cylindrically encapsulated PCM was developed using a machine learning algorithm. The data used for model training were extracted from the experimental study conducted by Fraiman et.al [20]. The predictions obtained from the machine learning model were compared with the correlation equation proposed by Fraiman et. al. After carefully testing the accuracy of the developed machine learning model, the geometric and thermal parameters were optimized using the genetic algorithm optimization method. Details about the problem definition, data processing, the machine learning algorithm used, and the optimization method are presented in the following subsections. Figure 1 presents the method used in this study.

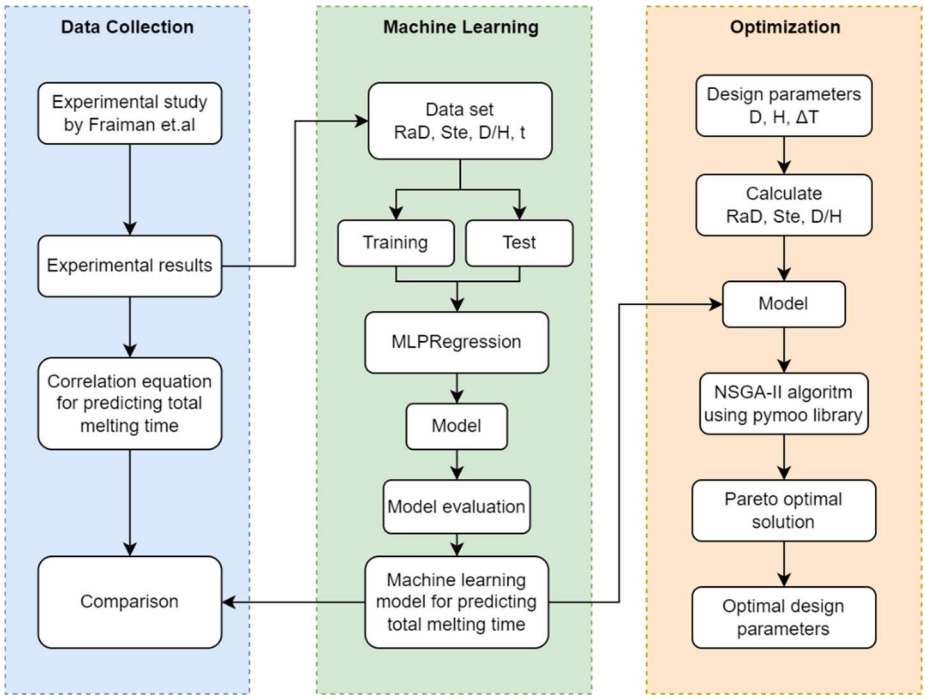

Figure 1. An overview of the methods utilized in this study

2.1. Problem Description

Figure 2 shows the schematic view of the melting problem of PCM in the cylinder. To investigate the effect of cylinder geometry and temperature difference on melting time, three different cylinder heights, four different cylinder diameters, and three different temperature differences were explored. In Fraiman's [20] experimental study, cylindrical tubes with diameters of 1, 2, 3, and 4 cm were used, while cylinder heights were 6, 12, and 17 cm. Experiments were conducted by maintaining the side surfaces of the cylinder at 10, 20, and 30 °C above the melting temperature of PCM. RT27 was used as the PCM. The thermophysical properties of the PCM are provided in Table 1.

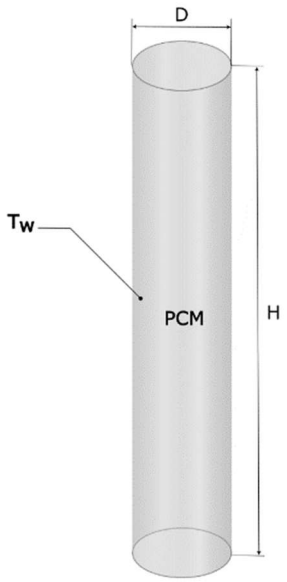

Figure 2. Schematic view of the PCM encapsulated in a vertical cylinder

Table 1. Thermophysical properties of the PCM [20]

Properties	RT27
ρ [kg/m^3]	781.6
C_p [kJ/kg^{o}C]	2.5
k [W/m^{o}C]	0.2
μ [kg/ms]	0.00392
T_m [^{o}C]	28 °C
L [kJ/kg]	179
β [1/K]	0.001

2.2. Data Processing

The results of the experimental study conducted by Fraiman et. al were extracted with the Webplotdigitizer tool. Thus, the total melting time of PCM was obtained for different diameter, height, and temperature difference conditions. When training the machine learning model, dimensionless numbers, such as Rayleigh and Stefan numbers, were utilized to establish a more generalized model and to compare it with experimental correlation results. Dimensionless numbers were calculated for each case, and the dataset used in machine learning was then created. Figure 3 illustrates the scatter matrix of the variables within the dataset.

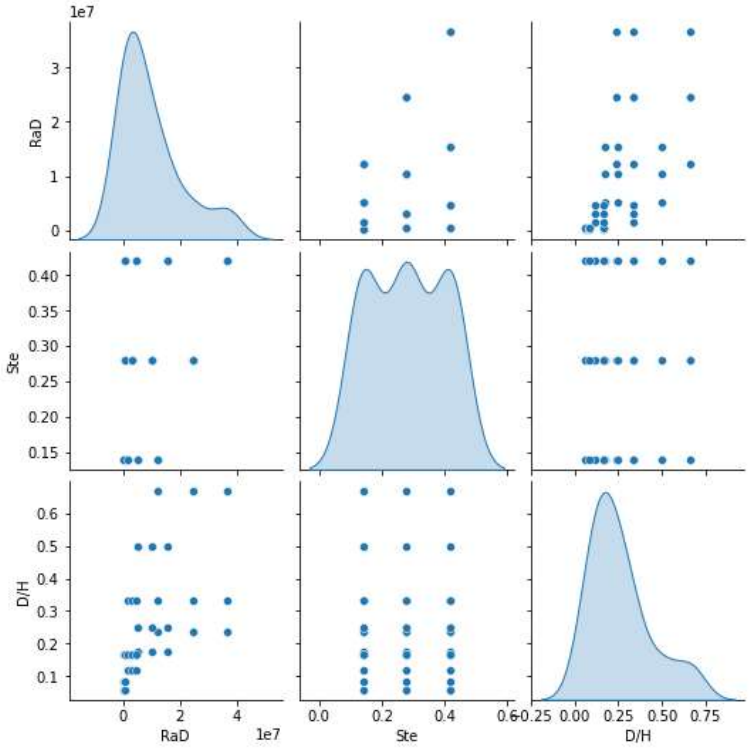

Figure 3. The scatter matrix of the variables

In order to express the effect of geometric and thermal parameters on the melting process of PCM with a generalized correlation, Fraiman proposed the following equation [20]:

$$MF = 1 - \left(1 - \frac{X}{1.3}\right)^{9/4} \quad (1)$$

where MF is melt fraction and X is defined as follows:

$$X = FoSte^{2/3}{Ra_D}^{1/5}(D/H)^{1/5} \quad (2)$$

where, Fo, Ste and Ra_D are Fourier, Stefan and Rayleigh numbers, defined as:

$$Fo = \frac{k}{\rho c_p}\frac{t}{D^2} \quad (3)$$

$$Ste = \frac{c_p \Delta T}{L} \quad (4)$$

$$Ra_D = \frac{g\rho^2 c_p \beta \Delta T D^3}{\mu k} \quad (5)$$

The Fourier number (Fo), Stefan number (Ste), and Rayleigh number (Ra) are dimensionless numbers used in heat transfer and fluid dynamics to characterize different physical phenomena. The Fourier number indicates the ratio of the rate of heat conduction to the rate of thermal energy storage. In phase change heat transfer, it helps determine how quickly heat is conducted through a material relative to the rate at which energy is stored in the material. The Stefan number quantifies the relative importance of sensible heat to latent heat during a phase change process. A higher Stefan number implies a greater proportion of sensible heat compared to latent heat. Lastly, the Rayleigh number describes the flow regime in buoyancy-driven flow. A high Rayleigh number indicates turbulent convection, while a low Rayleigh number indicates laminar flow.

Since a melting rate of 1 (MF=1) indicates complete melting, the total melting time can be calculated using the correlation equation proposed by Fraiman. Total melting times were calculated using this correlation equation with the same data to facilitate a comparison with the machine learning model.

2.3. Machine Learning Model

In the present investigation, a multilayer perceptron (MLP) network model was trained with the objective of predicting the total melting time of the PCM within a cylindrical enclosure.

The MLP, a widely utilized feed-forward backpropagation artificial neural network, comprises an input layer, at least one hidden layer, and an output layer. In each layer, the fundamental unit is referred to as a neuron, encompassing a summation unit and a non-linear activation function denoted as φ(x) [28,29]. The architecture of the developed model is shown in Figure 4.

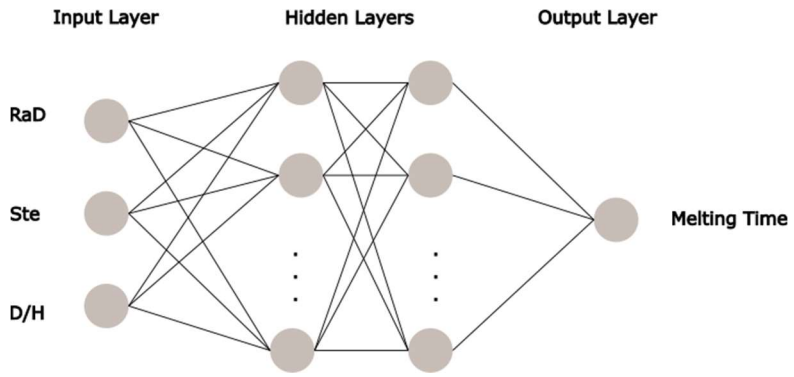

Figure 4. The architecture of the developed MLP model

Mathematical expressions (Eq. 6) can define the working principle of the neuron as a weighted sum of inputs, where the weights are multiplied by their corresponding input values, and the result is passed through a non-linear activation function [28,29].

$$y = \phi\left(\sum_{i=1}^{n}(w_i x_i) + b\right) \tag{6}$$

where, y is output of the neuron, φ is the activation function, w_i is the weight associated with input x_i, b is the bias term, n is the number of inputs.

Scikit-learn Python library [30] was used for model training. Scikit-learn is a widely used Python library for machine learning due to its comprehensive collection of algorithms and seamless integration with other libraries like NumPy and Pandas. It benefits from extensive documentation and a large, active community, making it an excellent choice for developing reliable and accurate machine learning models. In this study, the MLPRegressor function from the Scikit-learn library is utilized to train the model. The hidden layer sizes are set to (95, 36). The activation function is 'relu' and the solver is 'lbfgs'.

After preparing the dataset, Ra_D, Ste, and D/H were designated as input parameters, while melting time was assigned as the output parameter. Following the normalization of input parameters, 70% of the dataset was randomly allocated for training the model, and the remaining 30% was used for testing. For the model, two hidden layers, consisting of 90 and 36 neurons, were determined through a trial-and-error method. To evaluate the model's predictive accuracy, metrics such as the

coefficient of determination (R^2), mean absolute error (MAE), mean square error (MSE), and mean absolute percentage error (MAPE) were employed [30].

$$R^2(y,\hat{y}) = 1 - \frac{\sum_{i=1}^{n}(y_i - \hat{y}_i)^2}{\sum_{i=1}^{n}(y_i - \overline{y})^2} \tag{7}$$

$$\text{MAE}(y,\hat{y}) = \frac{1}{n_{\text{samples}}} \sum_{i=0}^{n_{\text{samples}}-1} |y_i - \hat{y}_i| \tag{8}$$

$$\text{MSE}(y,\hat{y}) = \frac{1}{n_{\text{samples}}} \sum_{i=0}^{n_{\text{samples}}-1} (y_i - \hat{y}_i)^2 \tag{9}$$

$$\text{MAPE}(y,\hat{y}) = \frac{1}{n_{\text{samples}}} \sum_{i=0}^{n_{\text{samples}}-1} \frac{|y_i - \hat{y}_i|}{max(\epsilon, |y_i|)} \times 100 \tag{10}$$

where $\hat{y}_i$ is predicted value, y_i and $\overline{y}$ are the corresponding true and mean values.

2.4. Optimization

In energy storage systems using PCM, the duration of energy storage (charging time) is as crucial as the amount of energy stored. In a cylindrically encapsulated PCM system, increasing the diameter or height of the cylinder can enhance the amount of stored energy. However, in this case, the melting time of PCM will also increase, resulting in a longer charging time for the system. Therefore, it is necessary to optimize the geometrical and thermal parameters to maximize energy storage in the shortest time.

The total amount of stored energy (E) can be expressed as the sum of sensible and latent heat:

$$E = m(L + c_p(T_w - T_m)) \tag{11}$$

where L is the latent heat of fusion, c_p is the specific heat, T_m is the melting temperature and T_w is the wall temperature of the cylinder. By dividing the total amount of stored energy (E) by the total

melting time (t) of the PCM, the amount of energy stored per unit time (mean power, P) can be expressed as follows.

$$P = E/t \tag{12}$$

The developed machine learning model and genetic optimization method are utilized to apply a multi-objective optimization, aiming to maximize both the amount of stored energy and power.

The NSGA-II [31] algorithm was selected for optimization, and the study was conducted using *pymoo*, an open-source Python library [32]. NSGA-II is designed specifically for multi-objective optimization problems, where the goal is to optimize multiple conflicting objectives simultaneously. The NSGA-II algorithm offers a powerful and versatile approach to multi-objective optimization problems, providing efficient exploration of the solution space, fast convergence to Pareto-optimal solutions, and robustness to changes in problem settings. These characteristics make NSGA-II a suitable choice for optimizing the objectives of this study, allowing for the identification of trade-offs and the selection of optimal solutions tailored to the specific needs of the problem domain. The algorithm begins by initializing a population of candidate solutions and evaluates each individual based on the defined objective functions. Using a non-dominated sorting mechanism, NSGA-II classifies individuals into different levels or fronts based on their dominance relationship, identifying Pareto-optimal solutions that are not dominated by any other solution. Crowding distance assignment ensures diversity among individuals within each front, guiding the selection process to favor solutions from less crowded regions of the objective space. Through a combination of genetic operators like crossover and mutation, NSGA-II generates offspring for the next generation while preserving diversity and exploring new regions of the search space. Elitist selection ensures that the best solutions from the previous generation survive, contributing to the convergence of the algorithm towards a diverse set of Pareto-optimal solutions. This iterative process continues until a termination condition is met, resulting in a well-distributed set of solutions representing trade-offs between conflicting objectives. In this study, the population size is set to 100, the offspring size is set to 10, and the termination criterion is set to 250 generations. The flowchart of the NSGA-II algorithm is presented in Figure 5.

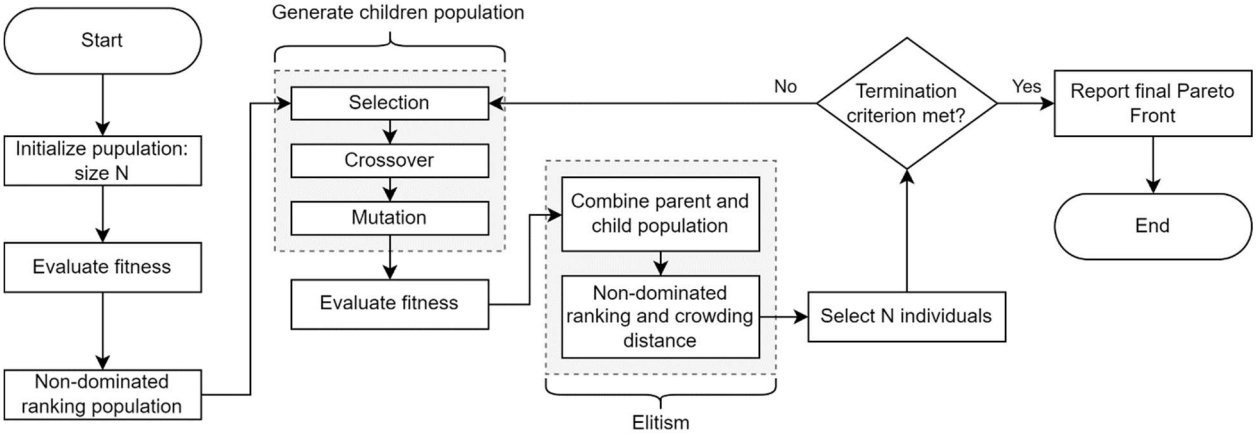

Figure 5. Flowchart of the NSGA-II algorithm

The parameters used in the optimization and their limits are provided in Table 2. While selecting these parameter ranges, the experimental data used in training the machine learning model were taken into account. Given the high accuracy of the trained model, the lower and upper limits of the parameters in the experimental study were slightly extended.

Table 2. Optimization parameters

Parameter	Ranges
D [cm]	0.75 – 5
H [cm]	5 – 20
ΔT [°C]	8 – 35

3. RESULTS

In this section, firstly, the prediction accuracy results of the machine learning model developed with the MLP method are presented. These results are then compared with the accuracy values of the correlation equation proposed by Fraiman et.al [20]. Subsequently, the optimization results using the developed model are presented.

3.1. Evaluation of Machine Learning Model for Melting Time Prediction

The melting time prediction accuracy results of the developed MLP model are presented in Table 3, compared with the correlation results proposed by Fraiman et al. [20]. The R^2 values for both the MLP model and the correlation results are relatively high, indicating a strong correlation between the predicted and actual values. Notably, the MLP model shows a slightly higher R^2,

suggesting better predictive performance. Moving on to the MAE values, which represent the average absolute difference between actual and predicted values, a lower MAE indicates better accuracy. In this case, the MLP model exhibits a significantly lower MAE, suggesting superior accuracy compared to the correlation results. Similarly, the MSE values, measuring the average squared difference between actual and predicted values, also favor the MLP model with a much lower MSE, indicating better overall performance compared to the correlation results. Examining MAPE, representing the average percentage difference between actual and predicted values, a lower MAPE indicates better accuracy. Here again, the MLP model demonstrates a significantly lower MAPE, implying better accuracy compared to the correlation results. In summary, based on the provided evaluation criteria, the MLP model consistently outperforms the correlation results from reference [20] across various metrics, demonstrating higher accuracy in predicting melting time.

Table 3. Comparison of Predictive Accuracy - MLP Model vs. Correlation Results (ref. **[**20])

Evaluation Criteria	MLP Model	Correlation [20]
R^2	0.9981	0.9749
MAE	0.370	1.957
MSE	0.5896	7.6654
MAPE (%)	4.07	16.68

To visually express the model's accuracy, predicted vs actual and predicted vs residuals plots for the entire dataset are shown in Figure 6 for the developed MLP model. Predicted vs actual and predicted vs residuals plots for the correlation of ref. [20] are presented in Figure 7. As seen in the figures, the maximum residual is 2.8 minutes for the developed MLP model, while the maximum residual of the correlation is 8 minutes. As evident, the developed MLP model successfully captures the relationship between the input parameters and the melting time, demonstrating high predictive accuracy.

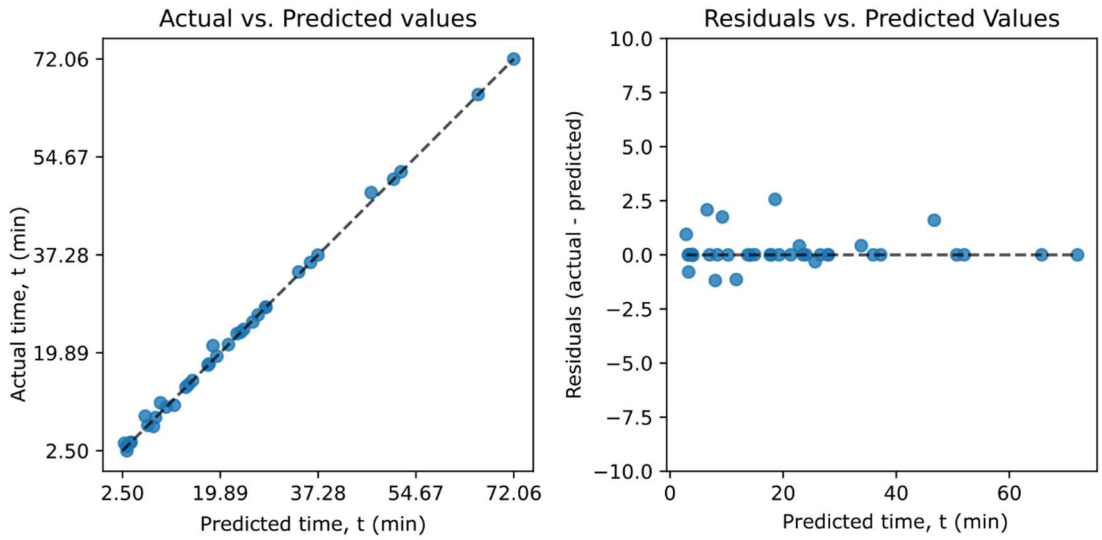

Figure 6. Melting time prediction performance of the developed MLP model

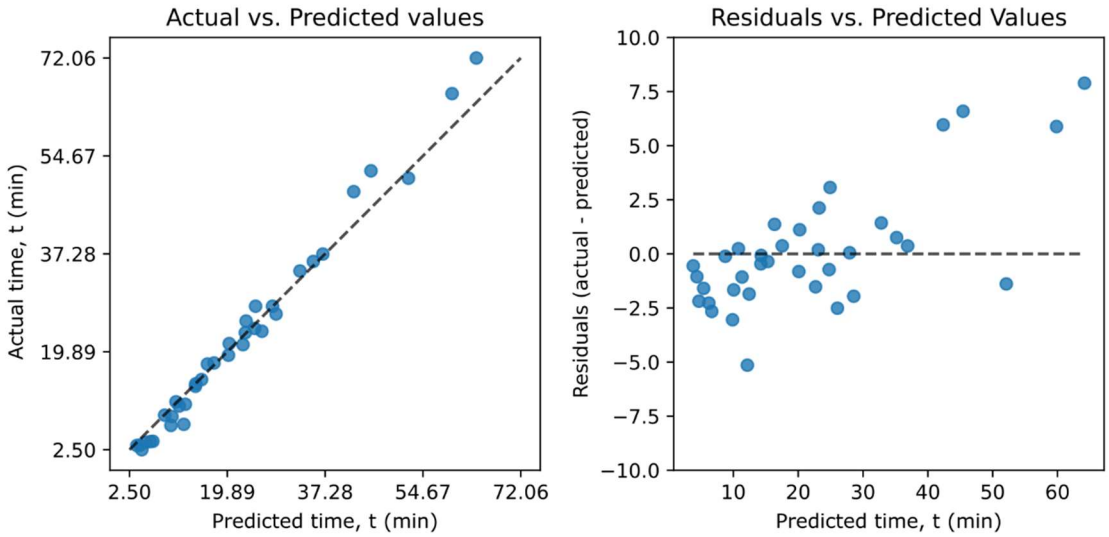

Figure 7. Melting time prediction performance of the correlation from ref. [20]

3.2. Optimization Results

To determine the optimal parameter combination maximizing both the amount of stored energy (E) and average power (P), the developed MLP model served as input for the NSGA-II algorithm. The resulting Pareto optimal solution is illustrated in Figure 8a, where each point represents an optimum solution. The weights assigned to the objective functions can guide the selection process from the optimal solution set. In scenarios where prioritizing the amount of stored energy is paramount, parameters that maximize energy can be selected from the solution set, resulting in minimum power. Conversely, opting for parameters that maximize power will minimize the stored

energy. In applications where both stored energy and power are equally important, both objective functions can be given equal weight. Figure 8b depicts the comparison of design points for the objectives of maximum stored energy, maximum power, and both objective functions with equal weight. For the objective of maximizing stored energy, the system achieved an energy storage of E = 81.78 kJ with a corresponding power of P = 12.69 W. In this scenario, the design parameters were determined as a diameter (D) of 5 cm, height (H) of 20 cm, and temperature difference (ΔT) of 35 °C. Conversely, in the pursuit of maximizing power, the system yielded a power of P = 73.38 W at the expense of stored energy, resulting in E = 37.10 kJ. The associated design parameters were determined as a diameter (D) of 3.4 cm, height (H) of 20 cm, and temperature difference (ΔT) of 35 °C. Lastly, under the scenario where both objectives were equally weighted, the system achieved a balance, with a power (P) of 38.89 W and stored energy (E) of 56.05 kJ. The corresponding design parameters included a diameter (D) of 4.1 cm, height (H) of 20 cm, and temperature difference (ΔT) of 35 °C.

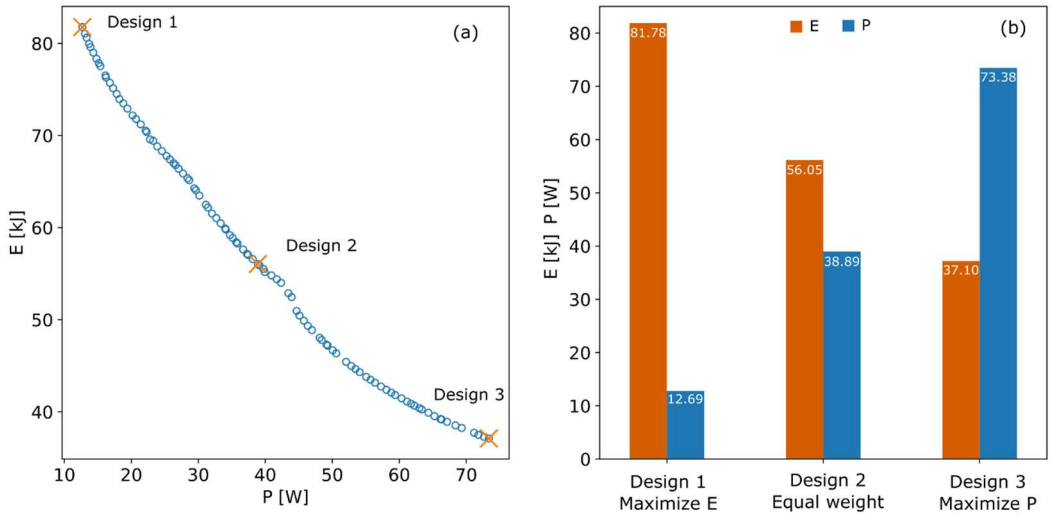

Figure 8. Pareto optimal solutions (a), comparison of the design points (b)

The accuracy of the optimized design points was tested by comparing the analytically calculated value of the stored energy with the value predicted by the machine learning model. For this purpose, the amount of energy stored was calculated analytically using Equation 11 with the diameter, height, and temperature difference values in Design 1, 2, and 3 cases. The comparison results are given in Figure 4. The largest error rate between the value predicted by the machine learning model and the analytically calculated value is 1.93% in Design 2. This error rate is smaller

than the model's MAPE value of 4.07%. It is evident that the model predicts the optimum design points with a minimal margin of error.

Table 4. Comparison of stored energy (E) for optimized design with analytical calculation.

Parameter	MLP Model, [kJ]	Analytical, [kJ]	Relative error, [%]
Design 1	81.78	81.79	0.01
Design 2	56.05	54.99	1.93
Design 3	37.10	37.82	1.90

4. CONCLUSIONS

In this study, a precise prediction model for the total melting time of cylindrically encapsulated PCM was developed employing a machine learning algorithm. The model's training data were sourced from an existing experimental study in the literature. A comparative analysis was conducted between the predictions generated by the machine learning model and the outcomes derived from the correlation equation. Following an assessment of the model's accuracy, the geometric and thermal parameters were optimized utilizing a genetic algorithm optimization method (NSGA-II). A summary of the conclusions is as follows:

- The developed MLP model outperformed the correlation equation proposed in the literature for predicting the total melting time. The MAPE value for the correlation equation in the literature is 16.68%, whereas the MAPE value for the developed MLP model is significantly lower at 4.07%. This significant difference indicates the success of the MLP model in capturing the relationship between input parameters and melting time.
- Optimization results indicate the need to establish a balance between the amount of stored energy and power during the design process. When the amount of stored energy is maximized (81.78 kJ), the power is minimized (12.69 W), and vice versa; when the power is maximized (73.38 W), the amount of stored energy is minimized (37.10 kJ).
- In the design with equal weighting for stored energy and power, the stored energy amounted to 56.05 kJ, and the power was 38.89 W. In this scenario, there is a 31.5% decrease in energy and a 206.5% increase in power compared to the design where energy is maximized. Additionally, there is a 44% decrease in power and a 51.1% increase in energy compared to the case where power is maximized.

These results collectively emphasize the robustness and effectiveness of the developed MLP model in accurately predicting melting time and providing optimal solutions for energy storage parameters, showcasing its potential for practical applications.

NOMENCLATURE

TES	thermal energy storage
PCM	phase change material
MLP	multilayer perceptron
MAE	mean absolute error
RMSE	root mean square error
MAPE	mean absolute percentage error
NSGA	non-dominated sorting genetic algorithm

DECLARATION OF ETHICAL STANDARDS

The author of the paper submitted declares that nothing which is necessary for achieving the paper requires ethical committee and/or legal-special permissions.

CONTRIBUTION OF THE AUTHORS

Burak İzgi: Conceptualization, Analysis; Methodology; Visualization; Writing - review & editing.

CONFLICT OF INTEREST

There is no conflict of interest in this study.

REFERENCES

[1] Palacios A, Barreneche C, Navarro ME, Ding Y. Thermal energy storage technologies for concentrated solar power–A review from a materials perspective. Renewable Energy 2020; 156: 1244–65.

[2] Enescu D, Chicco G, Porumb R, Seritan G. Thermal energy storage for grid applications: Current status and emerging trends. Energies 2020; 13: 340.

[3] Saffari M, de Gracia A, Fernández C, Belusko M, Boer D, Cabeza LF. Optimized demand side management (DSM) of peak electricity demand by coupling low temperature thermal energy storage (TES) and solar PV. Applied Energy 2018; 211: 604–16.

[4] Yang T, Liu W, Kramer GJ, Sun Q. Seasonal thermal energy storage: A techno-economic literature review. Renewable and Sustainable Energy Reviews 2021; 139: 110732.

[5] Guelpa E, Verda V. Thermal energy storage in district heating and cooling systems: A review. Applied Energy 2019; 252: 113474.

[6] Liu M, Riahi S, Jacob R, Belusko M, Bruno F. Design of sensible and latent heat thermal energy storage systems for concentrated solar power plants: Thermal performance analysis. Renewable Energy 2020; 151: 1286–97.

[7] Koçak B, Fernandez AI, Paksoy H. Review on sensible thermal energy storage for industrial solar applications and sustainability aspects. Solar Energy 2020; 209: 135–69.

[8] Alva G, Lin Y, Fang G. An overview of thermal energy storage systems. Energy 2018; 144: 341–78.

[9] Kalidasan B, Pandey AK, Shahabuddin S, Samykano M, Thirugnanasambandam M, Saidur R. Phase change materials integrated solar thermal energy systems: Global trends and current practices in experimental approaches. Journal of Energy Storage 2020; 27: 101118.

[10] Zhang N, Yuan Y, Cao X, Du Y, Zhang Z, Gui Y. Latent heat thermal energy storage systems with solid–liquid phase change materials: a review. Advanced Engineering Materials 2018; 20: 1700753.

[11] Wang X, Li W, Luo Z, Wang K, Shah SP. A critical review on phase change materials (PCM) for sustainable and energy efficient building: Design, characteristic, performance and application. Energy and Buildings 2022; 260: 111923.

[12] Arshad A, Jabbal M, Sardari PT, Bashir MA, Faraji H, Yan Y. Transient simulation of finned heat sinks embedded with PCM for electronics cooling. Thermal Science and Engineering Progress 2020; 18: 100520.

[13] Höhlein S, König-Haagen A, Brüggemann D. Macro-encapsulation of inorganic phase-change materials (PCM) in metal capsules. Materials 2018; 11: 1752.

[14] Farid M, Kim Y, Honda T, Kanzawa A. The role of natural convection during melting and solidification of PCM in a vertical cylinder. Chemical Engineering Communications 1989; 84: 43–60.

[15] Shmueli H, Ziskind G, Letan R. Melting in a vertical cylindrical tube: Numerical investigation and comparison with experiments. International Journal of Heat and Mass Transfer 2010; 53: 4082–91.

[16] Bechiri M, Mansouri K. Study of heat and fluid flow during melting of PCM inside vertical cylindrical tube. International Journal of Thermal Sciences 2019; 135: 235–46.

[17] Ebadi S, Tasnim SH, Aliabadi AA, Mahmud S. Melting of nano-PCM inside a cylindrical thermal energy storage system: Numerical study with experimental verification. Energy Conversion and Management 2018; 166: 241–59.

[18] Pan C, Charles J, Vermaak N, Romero C, Neti S, Zheng Y, et al. Experimental, numerical and analytic study of unconstrained melting in a vertical cylinder with a focus on mushy region effects. International Journal of Heat and Mass Transfer 2018; 124: 1015–24.

[19] Jones BJ, Sun D, Krishnan S, Garimella SV. Experimental and numerical study of melting in a cylinder. International Journal of Heat and Mass Transfer 2006; 49: 2724–38.

[20] Fraiman L, Benisti E, Ziskind G, Letan R. Experimental Investigation of Melting in Vertical Circular Tubes, Haifa, Israel: ASMEDC; 2008, 193–8.

[21] Mallya N, Haussener S. Buoyancy-driven melting and solidification heat transfer analysis in encapsulated phase change materials. International Journal of Heat and Mass Transfer 2021; 164: 120525.

[22] Verma TN, Nashine P, Singh DV, Singh TS, Panwar D. ANN: Prediction of an experimental heat transfer analysis of concentric tube heat exchanger with corrugated inner tubes. Applied Thermal Engineering 2017; 120: 219–27.

[23] Zhu S, Hrnjica B, Ptak M, Choiński A, Sivakumar B. Forecasting of water level in multiple temperate lakes using machine learning models. Journal of Hydrology 2020; 585: 124819.

[24] Jin W, Atkinson TA, Doughty C, Neupane G, Spycher N, McLing TL, et al. Machine-learning-assisted high-temperature reservoir thermal energy storage optimization. Renewable Energy 2022; 197: 384–97.

[25] Ren G, Chuttar A, Banerjee D. Exploring efficacy of machine learning (artificial neural networks) for enhancing reliability of thermal energy storage platforms utilizing phase change materials. International Journal of Heat and Mass Transfer 2022; 189: 122628.

[26] Amudhalapalli GK, Devanuri JK. Prediction of transient melt fraction in metal foam-nanoparticle enhanced PCM hybrid shell and tube heat exchanger: A machine learning approach. Thermal Science and Engineering Progress 2023; 46: 102241.

[27] Krishnayatra G, Tokas S, Kumar R. Numerical heat transfer analysis & predicting thermal performance of fins for a novel heat exchanger using machine learning. Case Studies in Thermal Engineering 2020; 21: 100706.

[28] Hinton GE. Connectionist learning procedures. Artificial Intelligence 1989; 40: 185–234.

[29] Li Y, Huang X, Huang X, Gao X, Hu R, Yang X, et al. Machine learning and multilayer perceptron enhanced CFD approach for improving design on latent heat storage tank. Applied Energy 2023; 347: 121458.

[30] Pedregosa F, Varoquaux G, Gramfort A, Michel V, Thirion B, Grisel O, et al. Scikit-learn: Machine Learning in Python. Journal of Machine Learning Research 2011; 12: 2825–30.

[31] Deb K, Pratap A, Agarwal S, Meyarivan T. A fast and elitist multiobjective genetic algorithm: NSGA-II. IEEE Trans Evol Computat 2002; 6: 182–97.

[32] Blank J, Deb K. Pymoo: Multi-Objective Optimization in Python. IEEE Access 2020; 8: 89497–509.